Paper No.
19306

AMPP ANNUAL CONFERENCE + EXPO
MARCH 19-23, 2023 | DENVER, COLORADO

Effect of Acetic Acid on Corrosion Product Layer Formation in Aqueous CO_2 Environments

Sahithi Ayyagari, Bruce Brown, Srdjan Nesic
Institute for Corrosion and Multiphase Technology, Ohio University
342 W State Street
Athens, Ohio, 45701
USA

ABSTRACT

The effect of the presence of acetic acid (HAc) on the formation of corrosion product layers in aqueous CO_2 environments was investigated using electrochemistry, weight loss, and extensive surface analysis procedures. Electrochemical tests (LPR, EIS, and potentiodynamic sweeps) were conducted in a 4 L glass cell with seven specimens of API 5L X65 steel - one for electrochemical measurements and six for surface analyses. Experiments were conducted in test solutions without organic acid and with 0.5 mM (30 ppm) undissociated HAc for ~240 h (10 days) and specimens were retrieved after 12 h, 120 h, and 240 h. The condition necessary for precipitation of iron carbonate, i.e., saturation level $S(FeCO_3)$ >1 was achieved by adding an external source of Fe^{2+} ions (de-oxygenated aqueous $FeCl_2$) at the beginning of the experiment. Modified thermodynamic calculations for the initial saturation value for iron carbonate, $S_{in}(FeCO_3)$, were used to compensate for complexation in experiments conducted in the presence of HAc. Surface and cross-sectional analysis were performed using XRD, SEM/EDS, and surface profilometry. It was observed that the corrosion product layers, formed without HAc and with 0.5 mM free HAc, remained protective, showing no indication of localized corrosion. The anodic and cathodic reactions of mild steel in solutions without HAc and with 0.5 mM free HAc were retarded by the formation of corrosion product layers indicating their protectiveness.

Key words: Complexation, acetic acid, CO_2 corrosion, localized corrosion, electrochemical measurements

INTRODUCTION

Several studies have focused in the past on the precipitation mechanism of iron carbonate ($FeCO_3$), which is the dominant corrosion product in CO_2 environments observed in the oil and gas industry. The dissolved CO_2 species undergo a series of chemical reactions and react with the oxidized iron ions forming $FeCO_3$ as the primary corrosion product. In the past, the thermodynamics of each of these reactions have been thoroughly studied and modified by incorporating the effects of temperature and non-ideality.

© 2023 Association for Materials Protection and Performance (AMPP). All rights reserved. No part of this publication may be reproduced, stored in a retrieval system, or transmitted, in any form or by any means (electronic, mechanical, photocopying, recording, or otherwise) without the prior written permission of AMPP.
Positions and opinions advanced in this work are those of the author(s) and not necessarily those of AMPP. Responsibility for the content of the work lies solely with the author(s).

The overall precipitation/dissolution reaction of $FeCO_3$ can be written as follows:

$$\boldsymbol{Fe^{2+}(aq) + CO_3^{2-}(aq) \rightleftharpoons FeCO_3(s)} \quad (1)$$

Net precipitation of $FeCO_3$ is observed when the solution becomes supersaturated with $FeCO_3$, i.e., when the solution exceeds the solubility limit of $FeCO_3$. Saturation value can be calculated using the following expression:

$$\boldsymbol{S(FeCO_3) = \frac{[Fe^{2+}][CO_3^{2-}]}{K_{sp}}} \quad (2)$$

where Ksp, the solubility product of iron carbonate, is a function of temperature (T) and solution ionic strength (I) [1]:

$$\boldsymbol{K_{sp} = 10^{-\left(-59.4-0.041377T_K-\frac{2.1963}{T_K}+24.5724\,log(T_K)+2.6349I^{0.5}-1.0027I\right)}} \quad (3)$$

$$\boldsymbol{I = \frac{1}{2}\sum_i c_i z_i^2} \quad (4)$$

where c_i is the concentration of each species in solution and z_i is the charge of the species.

The addition of organic acids to a pure CO_2 system complicates the water chemistry by inducing a change in pH and ionic strength, and formation of soluble complexes. Formation of soluble acetate complexes decreases the concentration of Fe^{2+} ions freely available, which decreases the bulk $S(FeCO_3)$ in the solution [2]. A previous study by Gulbrandsen et al. [2] has shown that as long as the solution is supersaturated, i.e. $S(FeCO_3)>>1$, protective corrosion product layers are formed regardless of the presence of HAc. Similar results have been reported in other studies, wherein, the presence of HAc merely delayed the formation of a protective $FeCO_3$ layer [3]. The feasibility and importance of formation of soluble acetate complexes, especially at higher temperatures, was explained in another study by Gulbrandsen et al. [4]. It was suggested that the driving force required for the formation of protective $FeCO_3$ films may become lower due to the formation of complexes. Equations for thermodynamic equilibrium constants for ferrous acetate complexes were obtained experimentally from a potentiometric titration study [5]; this previous study, conducted by Palmer et al. [5], further emphasized the need to review the water chemistry calculation with the addition of equilibrium constants for ferrous acetate complexes to better determine the concentration of freely available Fe^{2+} ions, especially at higher temperatures and higher concentrations of HAc.

The presence of organic acids may lead to instability in the $FeCO_3$ layer because of the changes in water chemistry. The influence of temperature and ionic strength on bulk solution pH, $S(FeCO_3)$, and $FeCO_3$ layer formation has received attention, leading to modification of the expression for solubility product. [1] However, despite the indications of the effects of complexation in the presence of organic acids, this effect has not been incorporated into corrosion product layer formation studies. This is an important area to focus upon in order to better understand the overall effect that organic acids have on the stability and formation of the $FeCO_3$ corrosion product layers.

In this context, thermodynamic calculations for corrosion product layer formation have been modified using equilibrium constants derived from Palmer et al.'s study [5] to compensate for complexation in experiments conducted in the presence of HAc. The present study aimed at understanding the protectiveness of the $FeCO_3$ corrosion product layers over longer exposures and the effect of HAc.

© 2023 Association for Materials Protection and Performance (AMPP). All rights reserved. No part of this publication may be reproduced, stored in a retrieval system, or transmitted, in any form or by any means (electronic, mechanical, photocopying, recording, or otherwise) without the prior written permission of AMPP.
Positions and opinions advanced in this work are those of the author(s) and not necessarily those of AMPP. Responsibility for the content of the work lies solely with the author(s).

EXPERIMENTAL

Equipment

Electrochemical tests were conducted in a 4-liter glass cell with seven specimens of API 5L X65 steel - one for electrochemical measurements and six for surface analyses. The corrosion specimens were flat, identical in size, with a working area of ~1.45 cm^2, and were located at the same radial distance from the center of the glass cell. The electrochemical specimen had an electrical connection established by soldering a copper wire to the back of the specimen, while the other specimens were simply immersed in the test solution. **Error! Reference source not found.** shows different parts of the experimental setup.

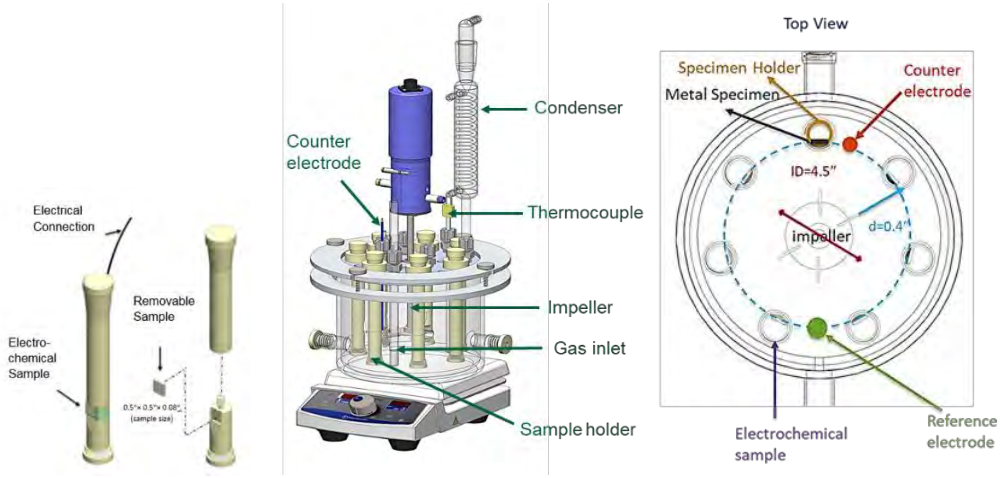

Figure 1. Experimental setup showing front view and top view of the glass cell

Test Matrix

Experiments were conducted in test solutions without organic acid and with 0.5 mM free HAc in a 1 wt.% NaCl solution de-aerated for at least 2 h with CO_2 sparging. The solution was continuously sparged with CO_2 and was maintained at 80°C and pH 6.6 throughout the duration of the experiment. The details of the test are shown in Table 1.

Table 1
Experimental parameters for layer forming conditions

Parameter	Conditions	
Temperature	80 ± 2 °C	
pH	6.60 ± 0.02	
pCO_2	0.53 bar	
Electrolyte	1 wt.% NaCl	
Flow condition	Quiescent	
Specimen	X-65 flat specimens (1.45 cm^2)	
Measurements	EIS for solution resistance (Rs) LPR for polarization resistance (Rp) Potentiodynamic sweeps for corrosion mechanisms	
$S_{in}(FeCO_3)$	~150	
$[Fe^{2+}]_{in}$	25 ppm	32 ppm
Total organic acid	0	27.8 mM HAc (1668 ppm)
Free HAc	0	0.5 mM (30 ppm)

© 2023 Association for Materials Protection and Performance (AMPP). All rights reserved. No part of this publication may be reproduced, stored in a retrieval system, or transmitted, in any form or by any means (electronic, mechanical, photocopying, recording, or otherwise) without the prior written permission of AMPP.
Positions and opinions advanced in this work are those of the author(s) and not necessarily those of AMPP. Responsibility for the content of the work lies solely with the author(s).

Calculations for concentration of acetate complexes

Dissociation of HAc:

$$HAc_{(aq)} \rightleftharpoons H^{+}_{(aq)} + Ac^{-}_{(aq)} \quad (5)$$

$$K_{HAc} = 10^{-\left(-6.661-0.0135*T_K+0.000238*(T_K)^2\right)} \quad (6)$$

Formation of $FeAc^{+}$ [5]:

$$Fe^{2+} + Ac^{-} \leftrightarrows FeAc^{+} \quad (7)$$

$$Q_1 = \frac{[FeAc^{+}]}{[Fe^{2+}][Ac^{-}]} \quad (8)$$

$$\log Q_1 = -\frac{4AI^{\frac{1}{2}}}{1+I^{\frac{1}{2}}} - \frac{10693}{T_K} - 55.283\ln(T_K) + 0.07924T_K + 328.05 - 10.384I + 0.010138T_K + \left(5.4101\times10^{-4}\right)I^2T_K + \frac{1426.8I^2}{T_K} + 13.706I\left\{\frac{\left(1+2I^{\frac{1}{2}}-2I\right)\exp\left(-2I^{\frac{1}{2}}\right)}{4I}\right\} \quad (9)$$

Formation of $FeAc_2$ [5]:

$$Fe^{2+} + 2Ac^{-} \leftrightarrows FeAc_2 \quad (10)$$

$$Q_2 = \frac{[FeAc_2]}{[Fe^{2+}][Ac]^2} \quad (11)$$

$$log\ Q_2 = -\frac{6AI^{\frac{1}{2}}}{1+I^{\frac{1}{2}}} - \frac{24890}{T_K} - 135.86\,ln(T_K) + 0.19611T_K + 800.73 + \frac{435.0681I}{T_K} - \left(3.1813\times10^{-3}\right)I^2T_K + \left(4.9867\times10^{-6}\right)T_K^2I \quad (12)$$

where, *A* is the Debye - Huckel parameter, and can be calculated as follows:

$$A = -2.97627 + 4.80688*10^{-2}T_K - 2.6928*10^{-4}T_K^2 + 7.49524*10^{-7}T_K^3 - 1.02352*10^{4}T_K^4 + 5.58004*10^{-13}T_K^5 \quad (13)$$

The total $[Fe^{2+}]$ present in the solution were measured using a spectrophotometer. A part of this measured $[Fe^{2+}]$ exists as complexes in the presence of HAc. The concentration of these complexes can be calculated using the above-mentioned expressions. The effective $[Fe^{2+}]$ that is available for the formation of $FeCO_3$ can be thus calculated as follows:

$$\left[Fe^{2+}\right]_{free} = \sum\left[Fe^{2+}\right]_{total} - [FeAc^{+}] - [FeAc_2] \quad (14)$$

For the present experimental conditions with 0.5 mM undissociated HAc at 80°C and pH 6.60, 32 ppm of $[Fe^{2+}]$ was added initially. This corresponds to an initial saturation of ~200. However, 11.23% of the

© 2023 Association for Materials Protection and Performance (AMPP). All rights reserved. No part of this publication may be reproduced, stored in a retrieval system, or transmitted, in any form or by any means (electronic, mechanical, photocopying, recording, or otherwise) without the prior written permission of AMPP.
Positions and opinions advanced in this work are those of the author(s) and not necessarily those of AMPP. Responsibility for the content of the work lies solely with the author(s).

total [Fe^{2+}] is present as $FeAc^{+}$ and 2.47% as $FeAc_2$. Therefore, the [Fe^{2+}] available for formation of $FeCO_3$ is ~ 27 ppm, which corresponds to $S_{in}(FeCO_3)$ of 150, same as that of the baseline experiments.

Electrochemical analysis methods

Electrochemical testing was performed using a Gamry[1] potentiostat and conducted twice for each experimental condition. The open circuit potential (OCP) (5 min) was measured for 5 min after introducing all the specimens, followed by electrochemical impedance spectroscopy (EIS) (20 min) and linear polarization resistance (LPR) (5 min). After an initial determination of corrosion potential, solution resistance and corrosion rate on the bare steel surface, a pre-calculated volume of de-aerated aqueous $FeCl_2$ was added to obtain a $S_{in}(FeCO_3)$ value of 150. The OCP and LPR tests were measured after every 1 hour over the duration of the test (240 h). A B-value of 26 mV/dec was used to calculate corrosion rates. At the end of layer formation tests (after 240 h), cathodic and anodic polarization was performed on the specimen for analysis of corrosion mechanisms. The details of the electrochemical analyses are defined in Table 2.

Table 2
Parameters for electrochemical measurements

Technique	Parameters	Results
Linear Polarization Resistance	Scan Rate: 0.125 mV / s. Polarization range: ± 5 mV (vs. OCP).	Polarization resistance (Rp)
Electrochemical Impedance Spectroscopy	Frequency range: 10000 Hz ~ 0.1 Hz. Amplitude: 10 mV. DC Potential: 0 vs. OCP	Solution resistance (Rs)
Potentiodynamic Sweeps	Scan Rate: 0.5 mV / s, Sampling period: 1 s Cathodic: 0 to -0.55 V (vs. OCP), Anodic: 0 to 0.15 V (vs. OCP)	Mechanisms

Experimental procedure

The specimens were metallographically polished using 180, 400 and 600 grit SiC abrasive papers; rinsed with DI water and isopropyl alcohol; dried and weighed before introducing into the test solution. The partial pressure of CO_2 was maintained by continuous sparging with CO_2 into solution and the temperature was controlled using a hot plate with thermocouple feedback. The pH was adjusted at the beginning of the experiments by adding small amounts of a de-oxygenated $NaHCO_3$ solution. The condition necessary for precipitation of iron carbonate, i.e., $S(FeCO_3)$ >1 was achieved by an adding external source of Fe^{2+} ions (de-oxygenated aqueous $FeCl_2$) at the beginning of the experiment. The layer forming experiments were started from the same initial saturation value of 150. The change in [Fe^{2+}] was measured by collecting solution specimens during the test. The corrosion behavior was studied *in situ* by electrochemical methods. Two specimens were retrieved after 12 h, 120 h, and 240 h; one of these specimens was used for surface analysis and the other for cross-sectional analysis.

[1] Trade name

© 2023 Association for Materials Protection and Performance (AMPP). All rights reserved. No part of this publication may be reproduced, stored in a retrieval system, or transmitted, in any form or by any means (electronic, mechanical, photocopying, recording, or otherwise) without the prior written permission of AMPP.
Positions and opinions advanced in this work are those of the author(s) and not necessarily those of AMPP. Responsibility for the content of the work lies solely with the author(s).

RESULTS AND DISCUSSION

Baseline conditions

Figure 2 shows the average values of LPR corrosion rates and corrosion potentials including the standard deviations of the four repeated experiments. It can be observed that the corrosion potential increased by ~90 mV in the first ~36 h while the corrosion rate reached a minimum value of ~0.1 mm/yr and remained the same for the rest of the test duration. This suggests that the corrosion product layers remained protective despite the observed decrease in the corrosion potential by some ~40 mV over the same period. The reason behind this observation needs to be explored further to better understand the properties of the corrosion product layers.

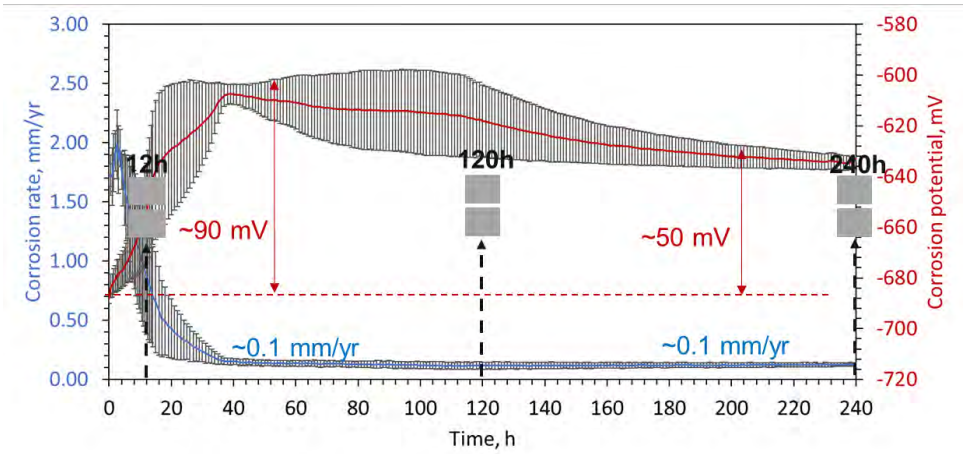

Figure 2. Variation of corrosion rate and corrosion potential with time in a 1 wt% NaCl solution in the absence of organic acids, with $S_{in}(FeCO_3)$ = 150, maintained at 80 °C, pH 6.60 over 240 hours

The specimens retrieved after 12 h, 120 h, and 240 h were analyzed to determine the surface and cross-sectional features of the corrosion product layers. The morphology of the specimen retrieved after 12h (Figure 3 (a)) shows the surface unevenly covered with $FeCO_3$ (prisms) and $Fe(CO_3)_2(OH)_2$ (plates) [6]. There appears to be a considerable area of the steel that was still actively corroding, as the corrosion rate at this time interval had not reached 0.1mm/yr. After 120h, he surface is observed to have an even coverage predominantly with $FeCO_3$ (prisms) (Figure 3 (b)) with traces of $Fe(CO_3)_2(OH)_2$ (plates). After 240 h, a uniform coverage with $FeCO_3$ can be observed (Figure 3 (c)).

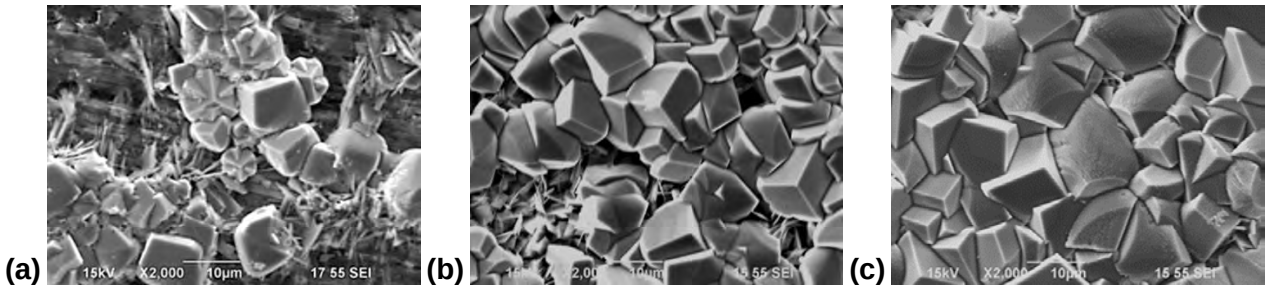

Figure 3. SEM micrographs of the corrosion product layer surface formed in a 1 wt% NaCl solution in the absence of organic acids, with $S_{in}(FeCO_3)$ = 150, maintained at 80 °C, pH 6.60 after (a) 12h , (b) 120h, and (c) 240h

The stacked XRD patterns of the specimens in Figure 3 are shown in Figure 4 and indicate that as time increased from 12h to 240 h, the intensity of the peaks corresponding to $FeCO_3$ increased, whereas the intensity of the peaks corresponding to $Fe(CO_3)_2(OH)_2$ and iron, α-Fe, decreased.

© 2023 Association for Materials Protection and Performance (AMPP). All rights reserved. No part of this publication may be reproduced, stored in a retrieval system, or transmitted, in any form or by any means (electronic, mechanical, photocopying, recording, or otherwise) without the prior written permission of AMPP.
Positions and opinions advanced in this work are those of the author(s) and not necessarily those of AMPP. Responsibility for the content of the work lies solely with the author(s).

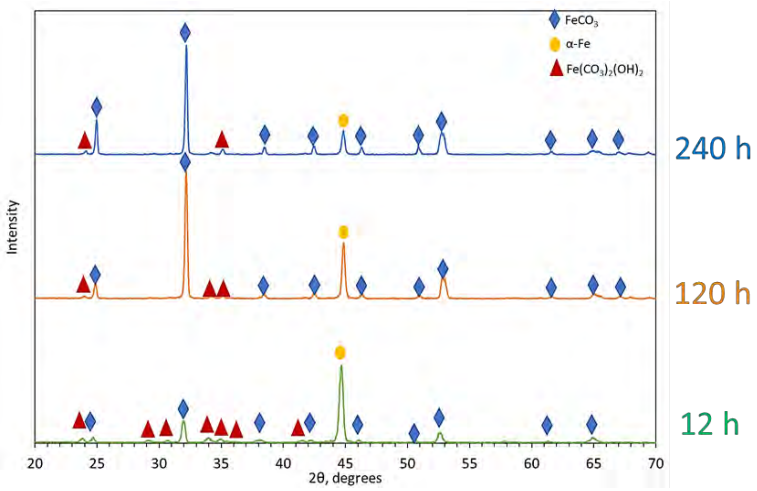

Figure 4. XRD patterns of the specimen surface formed in a 1 wt% NaCl solution in the absence of organic acids, with $S_{in}(FeCO_3)$ = 150, maintained at 80 °C, pH 6.60 after 12h , 120h, and 240h

The cross-section analysis of the specimens in Figure 5 shows the formation of a bi-layered corrosion product as discussed previously. The outer layer of the bi-layered corrosion product is believed to be the result of precipitation of $FeCO_3$ with Fe^{2+} originating from the solution, whereas the inner layer is the result of precipitation of $FeCO_3$ with Fe^{2+} originating from the corrosion of steel. This is an artefact of the experimental procedure which allowed corrosion of steel to progress, alongside the precipitation of $FeCO_3$ from the solution. Based on the weight loss of the specimens after corrosion product removal, the surface was observed to have receded by 1.6 µm, 4.8 µm, and 6.2 µm after 12 h, 120 h, and 240 h, respectively.

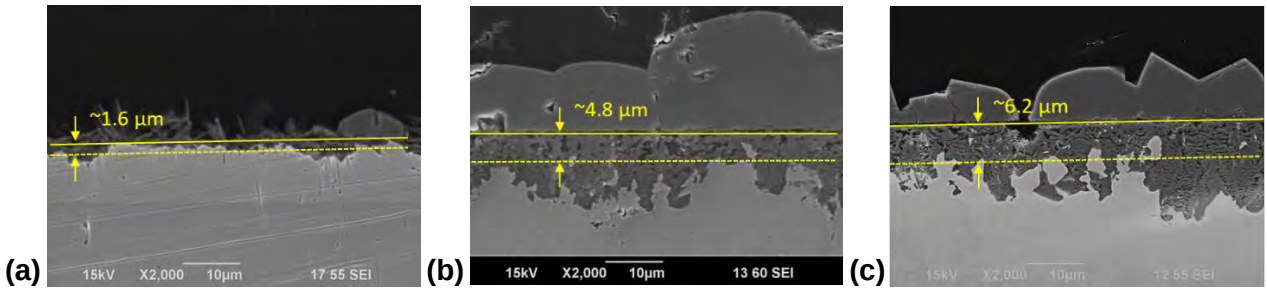

Figure 5. Cross-sections of the corrosion product layer formed in a 1 wt% NaCl solution in the absence of organic acids, with $S_{in}(FeCO_3)$ = 150, maintained at 80 °C, pH 6.60 after (a) 12 h , (b) 120 h, and (c) 240 h

While the average depth of the metal loss appears to be uniform in the 12 h specimen, the cross sections of the 120 h and 240 h specimens show regions of metal loss with greater depth of ~15 µm.

Profilometric scans conducted after the corrosion product layer removal shown in Figure 6 provide a more integrated perspective of the depth profile on the specimen surfaces. The profilometry scan of the 12 h specimen shows an average depth less than 2 µm (Figure 6a), clearly indicating that the specimen experienced uniform corrosion. The profilometry scan on the 120 h specimen reveals some indications of pitting initiation with pits greater than 10 µm (maximum pit depth of ~12 µm) and on the 240 h specimen shows a higher number initiated pits with more or less the same depth ~10 µm (maximum pit depth was ~15 µm). This suggests that although there are local areas indicating pitting corrosion initiation may have

© 2023 Association for Materials Protection and Performance (AMPP). All rights reserved. No part of this publication may be reproduced, stored in a retrieval system, or transmitted, in any form or by any means (electronic, mechanical, photocopying, recording, or otherwise) without the prior written permission of AMPP.
Positions and opinions advanced in this work are those of the author(s) and not necessarily those of AMPP. Responsibility for the content of the work lies solely with the author(s).

occured after 120 h of testing, the protectiveness of the corrosion product layer was not compromised as the depth of the pits did not increase significantly with time.

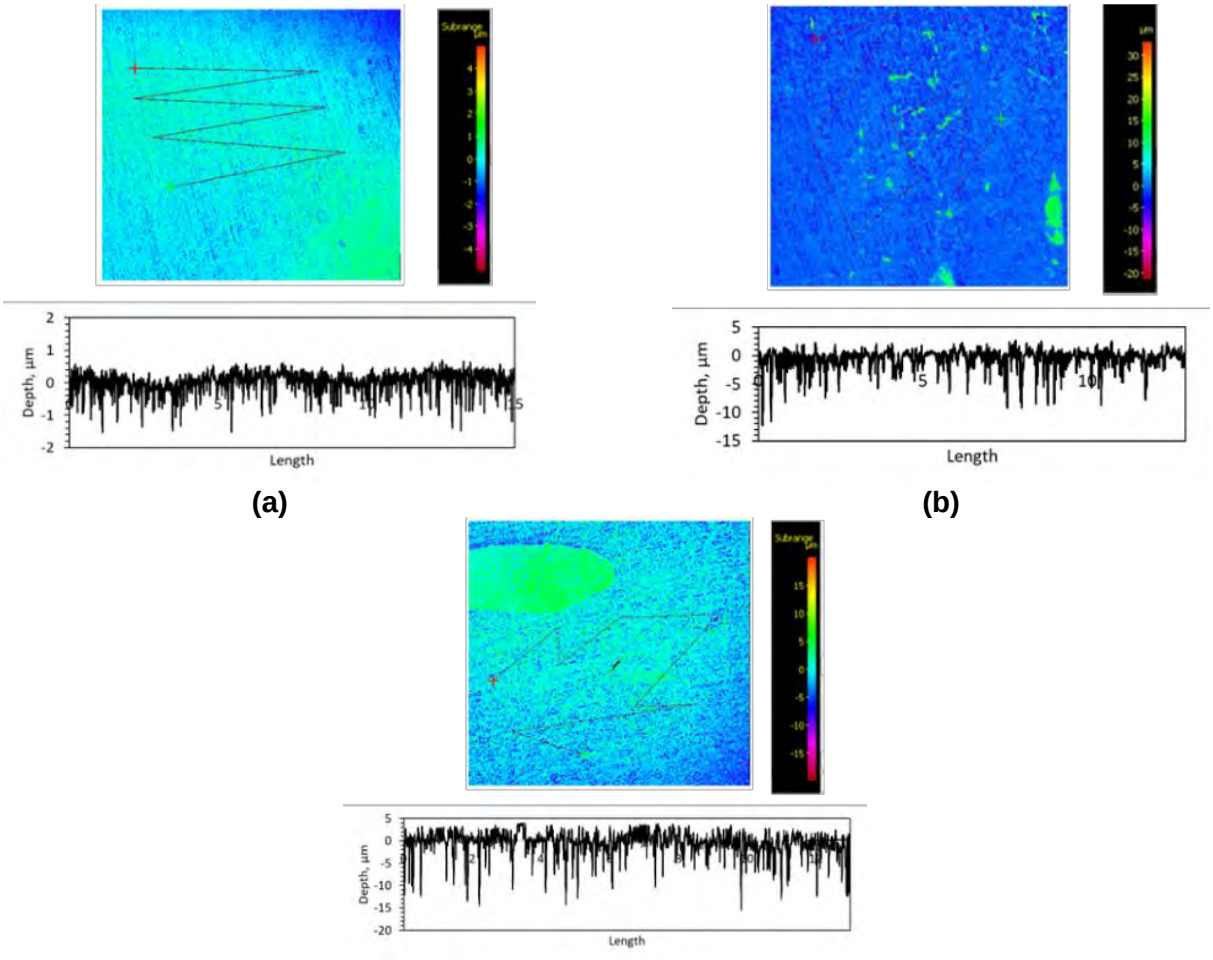

Figure 6. Profilometry scans of the specimen surface after the removal of the corrosion product layer formed in a 1 wt% NaCl solution in the absence of organic acids, with $S_{in}(FeCO_3)$ = 150, maintained at 80 °C, pH 6.60 after (a) 12 h , (b) 120 h, and (c) 240 h

These results clearly indicate that the corrosion product layers formed under the experimental conditions of $S_{in}(FeCO_3)$ = 150, 1 wt. % NaCl, maintained at 80 °C, pH 6.60, remain protective over 240 h (10 days) of testing.

The potentiodynamic sweeps performed on the steel surface before the corrosion product layer formation and after 240 h of testing are shown in Figure 7. It can be observed that the anodic reaction seems to have been retarded more than the cathodic reaction after the layer formation. The retardation of both the reactions hints at the reason behind the protectiveness of the corrosion product layers. This behavior needs to be studied further for conclusive understanding of the protectiveness of the corrosion product layers.

© 2023 Association for Materials Protection and Performance (AMPP). All rights reserved. No part of this publication may be reproduced, stored in a retrieval system, or transmitted, in any form or by any means (electronic, mechanical, photocopying, recording, or otherwise) without the prior written permission of AMPP.
Positions and opinions advanced in this work are those of the author(s) and not necessarily those of AMPP. Responsibility for the content of the work lies solely with the author(s).

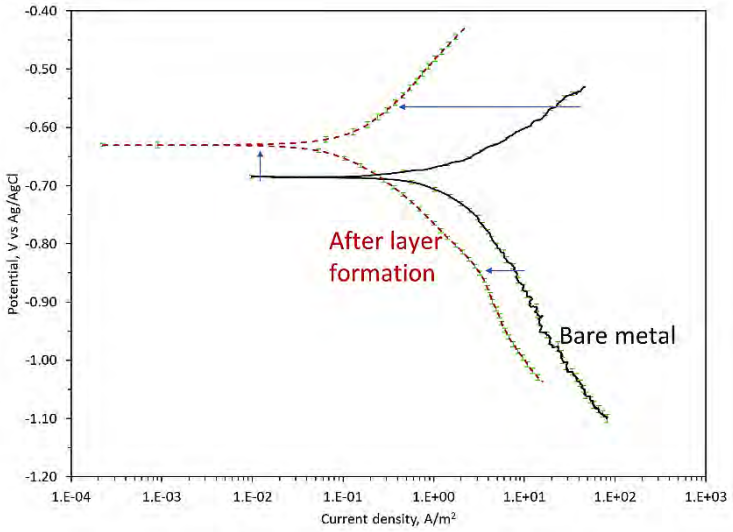

Figure 7. Potentiodynamic sweeps of steel in a 1 wt% NaCl solution in the absence of organic acids, with $S_{in}(FeCO_3)$ = 150, maintained at 80 °C, pH 6.60 before and after corrosion product layer formation

Effect of HAc

Figure 8 shows the average values of corrosion rates and corrosion potentials of two experiments containing 0.5 mM free HAc. As observed in the experiments without HAc, the corrosion rate reached a minimum value of ~0.1 mm/yr in ~40 h and remained the same for the rest of the test duration. This suggests that the corrosion product layers remained protective despite the decrease in the corrosion potential from by some ~20 mV over the same time.

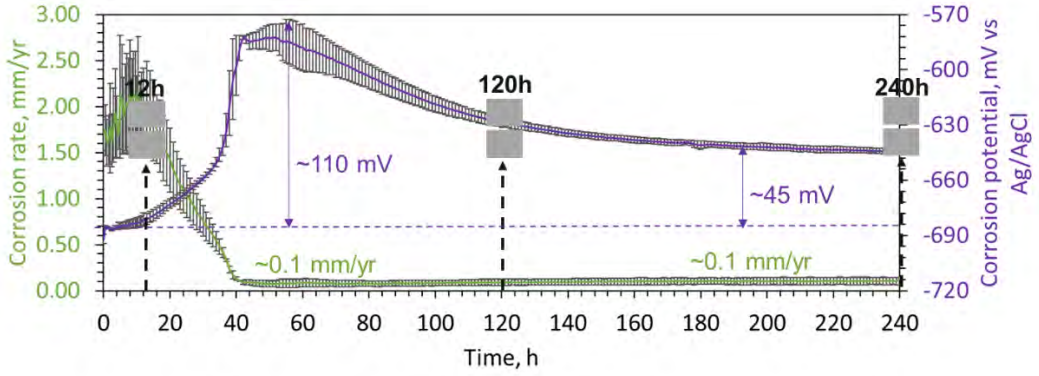

Figure 8. Variation of corrosion rate and corrosion potential with time in a 1 wt% NaCl solution in the presence of 0.5mM free HAc, with $S_{in}(FeCO_3)$ = 150, maintained at 80 °C, pH 6.60 over 240 hours

The specimens retrieved after 12 h, 120 h, and 240 h were analyzed to determine the surface and cross-sectional features of the corrosion product layers. As observed in the case of baseline conditions, the morphology of the specimen retrieved after 12 h (Figure 9a) shows the surface unevenly covered with $FeCO_3$ (prisms) and $Fe_2(OH)_2CO_3$ (plates). There appears to be a considerable area of the steel that is still actively corroding, as the corrosion rate at this time has not decreased to 0.1mm/yr. The surface is observed to have an even coverage with $FeCO_3$ (prisms) and $Fe_2(OH)_2CO_3$ (plates) after 120 h (Figure 9b). After 240 h, a uniform coverage with $FeCO_3$ can be observed (Figure 9c).

© 2023 Association for Materials Protection and Performance (AMPP). All rights reserved. No part of this publication may be reproduced, stored in a retrieval system, or transmitted, in any form or by any means (electronic, mechanical, photocopying, recording, or otherwise) without the prior written permission of AMPP.
Positions and opinions advanced in this work are those of the author(s) and not necessarily those of AMPP. Responsibility for the content of the work lies solely with the author(s).

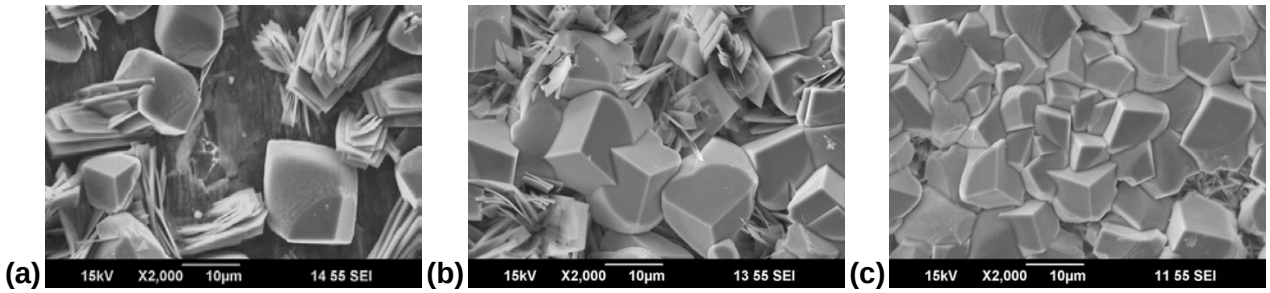

Figure 9. SEM micrographs of the corrosion product layer surface formed in a 1 wt% NaCl solution in the presence of 0.5mM free HAc, with $S_{in}(FeCO_3)$ = 150, maintained at 80 °C, pH 6.60 after (a) 12 h , (b) 120 h, and (c) 240 h

The stacked XRD patterns in Figure 10 of the specimens shown in Figure 9 indicate, as time increased from 12 h to 240 h, the intensity of the peaks corresponding to $FeCO_3$ increased, whereas the intensity of the peaks corresponding to $Fe_2(OH)_2CO_3$ and iron, α-Fe, decreased.

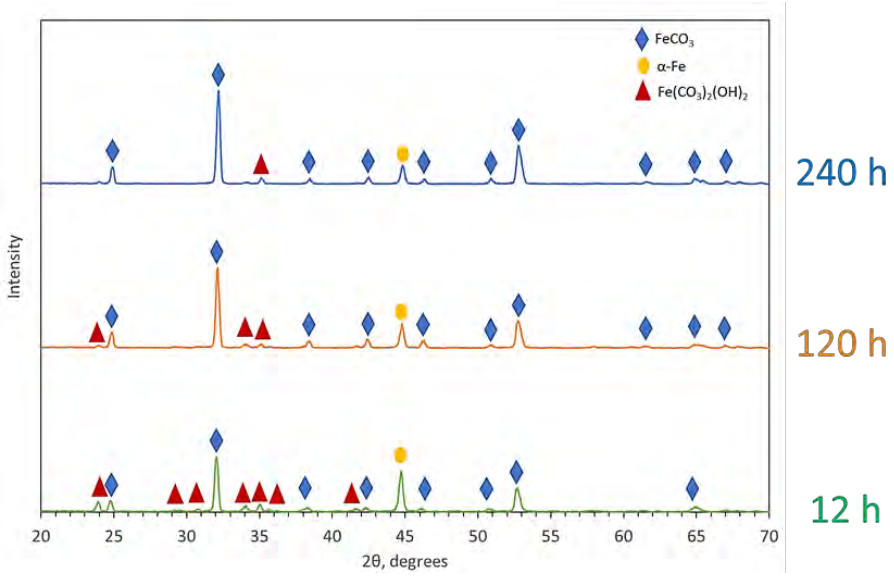

Figure 10. XRD patterns of the specimen surface formed in a 1 wt% NaCl solution in the presence of 0.5mM free HAc, with $S_{in}(FeCO_3)$ = 150, maintained at 80 °C, pH 6.60 after 12 h , 120 h, and 240 h

The cross-section analysis of the specimens shows the formation of a bi-layered corrosion product as shown in Figure 11. As time progressed, it can be observed that the thickness of the inner corrosion product layer and the outer precipitation layer increased. Based on the weight loss of the specimens after corrosion product removal, the surface was observed to have receded by 1.8 µm, 3 µm, and 3.5 µm after 12 h, 120 h, and 240 h, respectively. While the average depth of the metal loss appears to be uniform in the 12 h specimen, the cross sections of the 120 h and 240 h specimens show regions of metal loss with greater depth of ~16 µm.

© 2023 Association for Materials Protection and Performance (AMPP). All rights reserved. No part of this publication may be reproduced, stored in a retrieval system, or transmitted, in any form or by any means (electronic, mechanical, photocopying, recording, or otherwise) without the prior written permission of AMPP.
Positions and opinions advanced in this work are those of the author(s) and not necessarily those of AMPP. Responsibility for the content of the work lies solely with the author(s).

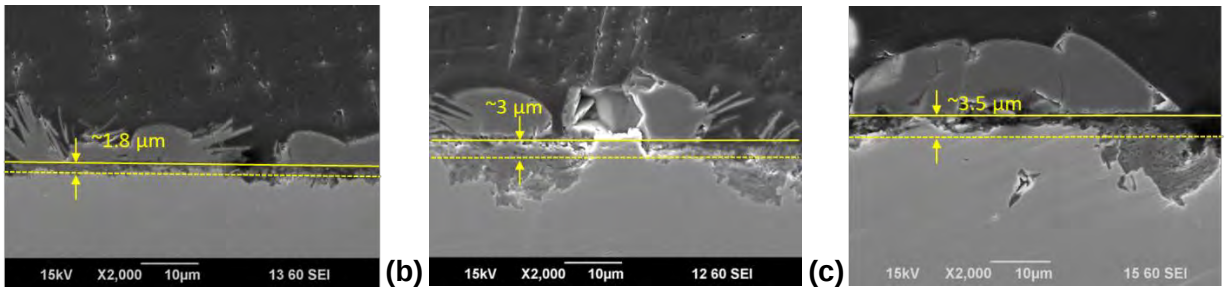

(a) (b) (c)

Figure 11. Cross-sections of the corrosion product layers formed in a 1 wt% NaCl solution in the presence of 0.5mM free HAc, with $S_{in}(FeCO_3)$ = 150, maintained at 80 °C, pH 6.60 after (a) 12 h , (b) 120 h, and (c) 240 h

Profilometric scans after corrosion product removal provided a more integrated perspective of the depth profile on the specimen surfaces. The profilometry scan of the 12 h specimen shows an average depth of ~1.5 µm, clearly indicating that the specimen was undergoing uniform corrosion. The scan on the 120 h specimen reveals a maximum pit depth of ~16 µm, and on the 240 h specimen shows a maximum pit depth of ~16 µm. This suggests that although there are local areas with deeper pits after 120 h of testing, the protectiveness of the corrosion product layer was not compromised as the depth of these pits did not increase significantly with time.

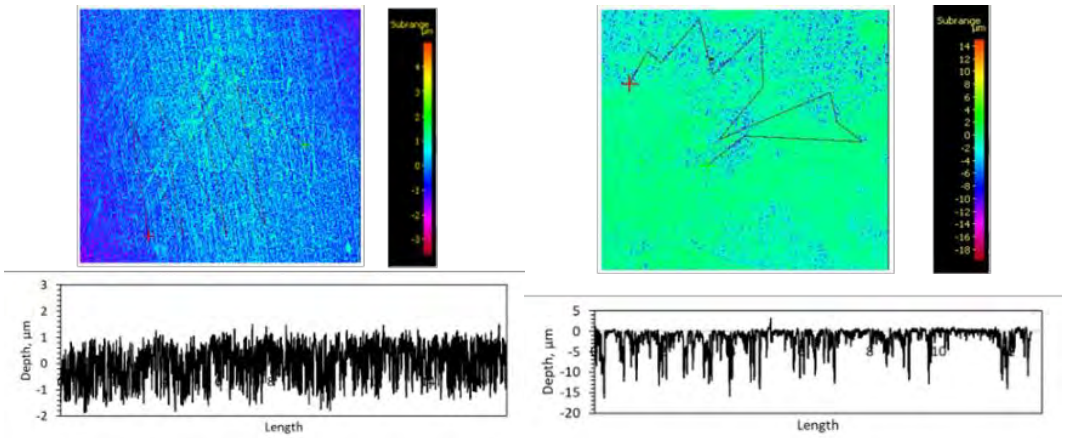

(a) (b)

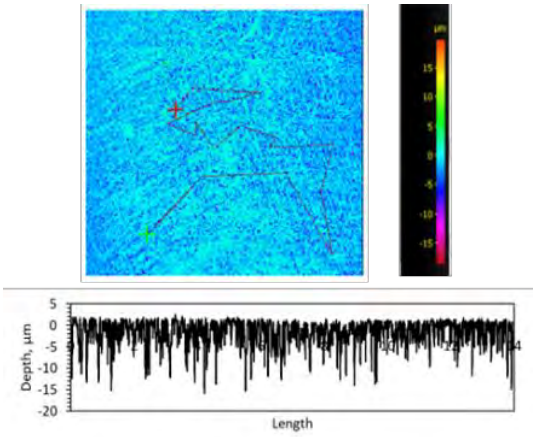

(c)

© 2023 Association for Materials Protection and Performance (AMPP). All rights reserved. No part of this publication may be reproduced, stored in a retrieval system, or transmitted, in any form or by any means (electronic, mechanical, photocopying, recording, or otherwise) without the prior written permission of AMPP.
Positions and opinions advanced in this work are those of the author(s) and not necessarily those of AMPP. Responsibility for the content of the work lies solely with the author(s).

Figure 12. Profilometry scans of the specimen surface after the removal of the corrosion product layer formed in a 1 wt% NaCl solution in the presence of 0.5mM free HAc, with $S_{in}(FeCO_3)$ = 150, maintained at 80 °C, pH 6.60 after (a) 12 h , (b) 120 h, and (c) 240 h

These results indicate that the corrosion product layers formed in the presence of 0.5mM free HAc under the experimental conditions of $S_{in}(FeCO_3)$ = 150, 1 wt. % NaCl, maintained at 80 °C, pH 6.60, remain protective over 240 h (10 days) of testing.

The potentiodynamic sweeps performed on the X65 steel in the presence of 0.5mM free HAc before the corrosion product layer formation and after 240 h of testing are shown in Figure 13. It can be observed that the anodic reaction seems to have retarded more than the cathodic reaction after the layer formation. The retardation of both the reactions indicates the reason behind the protectiveness of the corrosion product layers, however, this behavior needs to be studied further.

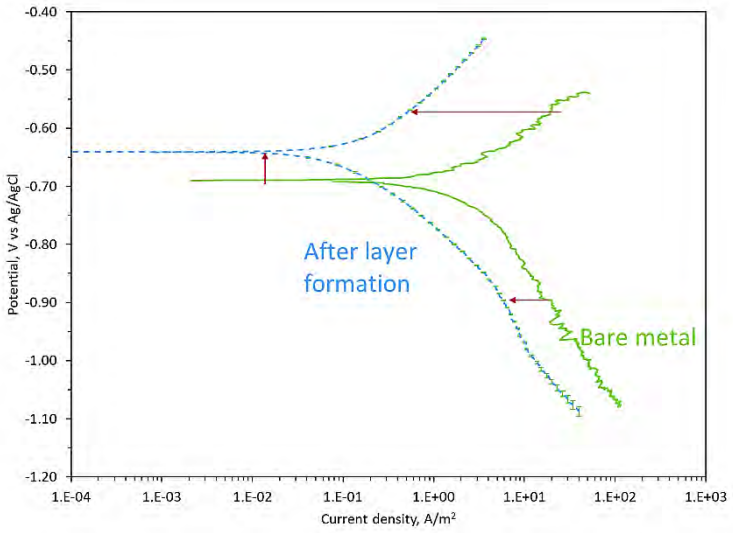

Figure 13. Potentiodynamic sweeps of steel in a 1 wt% NaCl solution in the presence of 0.5mM free HAc, with $S_{in}(FeCO_3)$ = 150, maintained at 80 °C, pH 6.60 before and after corrosion product layer formation

CONCLUSIONS

- The corrosion product layers formed, without HAc and with 0.5 mM free HAc, remained protective, showing no significant indication of localized corrosion.
- Both anodic and cathodic reactions, without HAc and with 0.5 mM free HAc, were observed to be retarded by the formation of corrosion product layers. This prompts the need for further investigation.

ACKNOWLEDGEMENTS

The author would like to thank the following companies for their financial support:
Ansys, Baker Hughes, Chevron Energy Technology, Clariant Corporation, ConocoPhillips, ExxonMobil, M-I SWACO (Schlumberger), Multi-Chem (Halliburton), Occidental Oil Company, Pertamina, Saudi Aramco, Shell Global Solutions and TotalEnergies.

© 2023 Association for Materials Protection and Performance (AMPP). All rights reserved. No part of this publication may be reproduced, stored in a retrieval system, or transmitted, in any form or by any means (electronic, mechanical, photocopying, recording, or otherwise) without the prior written permission of AMPP.
Positions and opinions advanced in this work are those of the author(s) and not necessarily those of AMPP. Responsibility for the content of the work lies solely with the author(s).

REFERENCES

[1] Z. Ma, X. Gao, B. Brown, S. Nesic and M. Singer, "Improvement to water speciation and $FeCO_3$ precipitation kinetics in CO_2 environments: Updates in NaCl concentrated solutions," Industrial and Engineering Chemistry Research, 60 (47), pp. 17026−17035, 2021.

[2] E. Gulbrandsen, “Acetic acid and carbon dioxide corrosion of carbon steel covered with iron carbonate,” *CORROSION NACE International*, Paper no. 07322, pp. 1–22, 2007.

[3] O. A. Nafday and S. Nesic, “Iron carbonate scale formation and CO_2 corrosion in the presence of acetic acid,” *CORROSION NACE International*, Paper no. 05295, pp. 1 - 27, 2005.

[4] K. Bilkova and E. Gulbrandsen, “Solution chemistry effects on corrosion of carbon steels in presence of CO_2 and acetic acid,” *CORROSION NACE International*, Paper no. 06364, pp. 1–37, 2006.

[5] D. A. Palmer and S. E. Drummond, “Potentiometric determination of the molal formation constants of ferrous acetate complexes in aqueous solutions to high temperatures,” *Journal of Physical Chemistry*, Vol. 92, pp. 6795–6800, 1988.

[6] A. Michelin, E. Leroy, D. Neff, J. J. Dynes, P. Dillmann, and S. Gin, “Archeological slag from Glinet: An example of silicate glass altered in an anoxic iron-rich environment,” *Chemical Geology*, vol. 413, pp. 28–43, 2015

© 2023 Association for Materials Protection and Performance (AMPP). All rights reserved. No part of this publication may be reproduced, stored in a retrieval system, or transmitted, in any form or by any means (electronic, mechanical, photocopying, recording, or otherwise) without the prior written permission of AMPP.

Positions and opinions advanced in this work are those of the author(s) and not necessarily those of AMPP. Responsibility for the content of the work lies solely with the author(s).